北海道教育大学紀要（自然科学編）第59巻　第１号　　平成20年８月
Journal of Hokkaido University of Education (Natural Sciences) Vol. 59, No.1　　August, 2008

OZI-Allowed Decays and Structure of ψ-States

HIRANO Masanobu, MATSUDA Yasuo * and SAKAI Motoki **

Department of Physics, Sapporo Campus, Hokkaido University of Education, Sapporo 002-8502

*Faculty of Dairy Science, Rakuno Gakuen University, Ebetsu 069-8501

**Department of Physics, Asahikawa Campus, Hokkaido University of Education, Asahikawa 070-8621

OZI 許容崩壊とψ-状態の構造

平野　雅宣・松田　康夫*・酒井　源樹**

北海道教育大学札幌校物理学教室

*酪農学園大学酪農学部

**北海道教育大学旭川校物理学教室

ABSTRACT

A nonrelativistic coupled-channel model based on microscopic effective quark interactions is used to study the masses and OZI-allowed partial decay widths of ψ-states. Considering our neglect of spin dependent forces, the numerical result is very successful and encouraging for the traditional ψ-states. In particular, the ψ(4040)'s features of mass and partial decay widths, which have been viewed with great attention historically, are reproduced well. Although it is dominantly in $c\bar{c}$ S-wave and can be assigned as ψ(3S), it was found to become a $D^*\bar{D}^*$ continuum state when the open channel coupling is switched off, while, the ψ(2D) and ψ(4S) states are reduced to the unperturbed $c\bar{c}$ $3S$ and $2D$-states respectively when the coupling is off. Model solutions other than the traditional ψ-states appear and some of them are discussed in relation with new particles observed recently.

1 Introduction

Importance of the nodal structure of ψ-states wave-functions was noted[1),2)] first by the Orsay group in the analysis[3)] of OZI-allowed decays.[4)] The harmonic oscillator model was used for the mass spectrum and the $^3P_0$ model[5)] for the decay vertex. That is, mass and decay dynamics were treated separately. Soon after, the Cornell group proposed a unified treatment of mass and decay based on effective quark interactions showing the QCD features.[6)] Their numerical results, however, turned out to be not so satisfactory. Recently, the Cornell group reported that their model happened to produce good numerical results[7)] by using a different value of string tension from that chosen previously.

We have slightly modified[8)] the Cornell model by introducing the one boson exchange interaction in channels between the charmed meson and the anti-charmed meson. We set up a coupled channel equation with the linear plus Coulomb potential in the $c\bar{c}$ channels, OBE potentials in the open decay channels and transition potentials in the off diagonal parts of the potential connecting the two channels. A solution of the $c\bar{c}$ channels without the decay coupling is a bound state without any decay width. A solution of the latter system without coupling is that of either a continuum state or an unbound S-matrix pole state with a large decay width. By the coupling of these channels, bound states, resonant- and pole-states other than continuum states are brought about. That is, a heavy quark-antiquark pair-state below open decay channels stays as a bound state, the one above open channel thresholds obtains a decay width and becomes a resonant state, and some of pole states with wide width and continuum states can be pole states with comparatively narrow widths. When the total width of some of these pole states is narrow, the state can be an observable resonant state.

The coupled channel equation was transformed by the complex coordinate scale rotation[9] and then we solved the transformed coupled channel equation numerically. Using the framework, mass spectra and total decay widths of ψ's[8] and Υ's.[10] have previously been studied. The partial decay width analysis needs more detailed knowledge of the wave functions and therefore, reliability of the present framework is tested in details by this analysis.

2 Brief survey of our coupled channel framework

In this section we briefly outline our coupled-channel model. For details, refer to Ref. 8) of Yabusaki et al. In this paper, we only deal with the $J^{PC} = 1^{--}$ ψ-states. Our coupled-channel equation consists of the confined $c\bar{c}$ channels and the 6 open meson-antimeson channels. The formers are two confined $c\bar{c}$ channels, one with the relative orbital angular momentum $L = 0$ and the other with $L = 2$. The latter open channel states we consider are those shown in Table I. Among them, the $\mathrm{D^*\bar{D}^*}$- and $\mathrm{D_s^*\bar{D}_s^*}$-channels have two relative orbital angular momenta $l = 1, 3$ and the others $l = 1$. These heavy mesons in the open channels are treated as elementary ones.

The radial part of our coupled channel equation is written as in the following form;

$$\mathcal{H}\Psi(r) = \left\{\mathcal{T}(r) + \mathcal{V}(r)\right\}\Psi(r) = E\Psi(r). \tag{1}$$

Here $\mathcal{T}(r)$ and $\mathcal{V}(r)$ are the kinetic and potential energy operators, respectively;

$$\mathcal{T}(r) = \begin{pmatrix} -\dfrac{1}{2\mu_0}\dfrac{\mathrm{d}^2}{\mathrm{d}r^2} & 0 \\ 0 & -\dfrac{1}{2\mu}\dfrac{\mathrm{d}^2}{\mathrm{d}r^2} \end{pmatrix} \tag{2}$$

and

$$\mathcal{V}(r) = \begin{pmatrix} G(r) + \dfrac{L(L+1)}{2\mu_0 r^2} & f(r) \\ f^{\mathrm{T}}(r) & Y(r) + \dfrac{l(l+1)}{2\mu r^2} \end{pmatrix}, \tag{3}$$

where μ_0 is the reduced masses of the $(c, \bar{c})$ system. The matrix μ^{-1} represents a diagonal matrix whose diagonal elements are given by reduced masses $1/\mu_j$ of the j-th open channel in Table I.

Table I: Open channels of the meson-antimeson taken into account in the present analysis

j (Channel no.)	Open channel
1	$\mathrm{D\bar{D}}$
2	$(\mathrm{D\bar{D}^*} + \mathrm{D^*\bar{D}})/\sqrt{2}$
3	$\mathrm{D^*\bar{D}^*}$
4	$\mathrm{D_s\bar{D}_s}$
5	$(\mathrm{D_s\bar{D}_s^*} + \mathrm{D_s^*\bar{D}_s})/\sqrt{2}$
6	$\mathrm{D_s^*\bar{D}_s^*}$

The potential $G(r)$ in the $c\bar{c}$ channel is of the standard linear plus Coulombic type,

$$G(r) = \lambda r + b - \frac{\alpha}{r}, \tag{4}$$

where λ, b and α are the string tension, a constant potential and one-gluon exchange constant of QCD, respectively. Extending this potential, an effective quark interaction has been considered;[6),11)]

$$H_{\mathrm{int}} = \frac{3}{8}\int \mathrm{d}^3\boldsymbol{x}\,\mathrm{d}^3\boldsymbol{x'}\,\bar{\psi}_{f'}(\boldsymbol{x'})\,\Gamma_i\frac{\lambda^a}{2}\psi_{f'}(\boldsymbol{x'})\,V_i(|\boldsymbol{x'}-\boldsymbol{x}|) \times\bar{\psi}_f(\boldsymbol{x})\,\Gamma_i\frac{\lambda^a}{2}\,\psi_f(\boldsymbol{x}). \tag{5}$$

The $\psi_f(\boldsymbol{x})$ stands for the quark field operator with the flavor f. It is a vector in color degree of freedom and λ^a's are the color SU(3) generators. Γ_i is either the γ matrix or the unit matrix depending on Lorentz property (vector or scalar) of the $V_i(r)$. As $V_i(r)$ $(i = 1, 2)$, we take the Coulombic potential and the linear plus constant potential, both transforming as Lorentz vector in this article;

$$V_1(r) = -\frac{\alpha}{r}, \qquad V_2(r) = \lambda r + b, \tag{6}$$

where $G(r) = V_1(r) + V_2(r)$. By this effective interaction Hamiltonian, mass and decay of heavy quarkonium states,[6] the quark condensation[11] and the chiral symmetry breaking[12] have been studied.

The $f(r)$ is the transition potential connecting the $c\bar{c}$ channels and the heavy meson-antiheavy meson channels. The explicit form $f(r)$ based on Eq. (5) is given in Ref. 8). The $Y(r)$ is the heavy meson-antiheavy meson potential.

A ψ-state is expressed by a multi-component wave function $\Psi(r)$ as a sum of closed quark-antiquark components $b(r)$ and open meson-antimeson components $u_j(r)$:

$$\Psi(r) = \sum_L b^L(r) + \sum_{j,l} u^l_j(r). \tag{7}$$

In this article, we consider mainly 1^{--} ψ-states of $\psi(1S)$–$\psi(4S)$, $\psi(1D)$ and $\psi(2D)$.

Now we briefly explain the formulae for evaluating partial decay widths that have been discussed by Moiseyev and Peskin.[13] Their formulae are based on the complex (coordinate) scale transformation[9] of the relative coordinate of the two-particle system to the complex plane;

$$U(\theta) : r \rightarrow r\mathrm{e}^{\mathrm{i}\theta}. \tag{8}$$

Then the coupled-channel equation is expressed as

$$\mathcal{H}(\theta)\Psi_\theta(r) = E_\theta \Psi_\theta(r), \tag{9}$$

where $\mathcal{H}(\theta) = U(\theta)HU(\theta)^{-1}$, and $\Psi_\theta(r) = U(r)\Psi(r)$. Since $\mathcal{H}(\theta)$ is not hermitian, eigenvalues E_θ are not real. According to the so-called ABC-theorem,[9] the bound and resonant states have θ-independent real (negative) and complex eigenvalues, respectively. The real and imaginary parts of the complex resonant eigenvalue $E^{\mathrm{r}}_\theta = M - \mathrm{i}\Gamma/2$ stand for mass and a half of total decay width of the system. The eigenvalue E^{r}_θ is independent of θ if $\theta \geq \tan^{-1}(\Gamma/2M)$. The solutions of unbound states have continuous complex energy $E^{\mathrm{c}}_\theta = E_{\mathrm{r}} + \mathrm{i}E_{\mathrm{i}}$ on the 2θ-rotated branch cut.

The merit of this method is that resonant-state solutions can be obtained by the same method as bound-state solutions in the L^2 integrable functions. It has been applied to systems in the field of atomic and molecular physics and then to nuclear physics. Subsequently, the method was applied to mass and total decay width evaluation of ψ's[8] and Υ's.[10] In the coupled channel framework, a resonance wave function $\Psi(r)$ is written as a superposition of closed quark-antiquark components $b(r)$ and open meson-antimeson components $u_j(r)$ as in Eq. (7). As shown in the Ref. 13), the ratio of the partial widths Γ_j and $\Gamma_{j'}$ of decay of a heavy quarkonium state ψ to open channels j and j' in Table I, respectively, is given by

$$\Gamma_j/\Gamma_{j'} = \sum_l \left|a^l_j\right|^2 \Big/ \sum_{l'} \left|a^{l'}_{j'}\right|^2, \tag{10}$$

where a^l_j is the complex-scaled flux amplitude of the j-th open channel component at an asymptotic region of r where only the outgoing component exists.

$$u^l_j(r\mathrm{e}^{\mathrm{i}\theta}) \overset{r\to\infty}{\longrightarrow} a^l_j\,\phi(r\mathrm{e}^{\mathrm{i}\theta}), \tag{11}$$

$$\phi(r\mathrm{e}^{\mathrm{i}\theta}) = \sqrt{\frac{\mu_j}{\hbar k_j}}\mathrm{e}^{\mathrm{i}k_j(r\mathrm{e}^{\mathrm{i}\theta})}, \tag{12}$$

where $\phi(r\mathrm{e}^{\mathrm{i}\theta})$ is normalized to a unit current density. The expression (10) is rewritten in terms of the wavefunctions $u_j(r)$ as

$$\frac{\Gamma^l_j}{\Gamma^{l'}_{j'}} = \lim_{r\to\infty}\left|\frac{(k_j)^{1/2}\mu_{j'}u^l_j(r\mathrm{e}^{\mathrm{i}\theta})}{(k_{j'})^{1/2}\mu_j u^{l'}_{j'}(r\mathrm{e}^{\mathrm{i}\theta})}\mathrm{e}^{\mathrm{i}(k_{j'}-k_j)r\mathrm{e}^{\mathrm{i}\theta}}\right|^2 \equiv \lim_{r\to\infty} R^{jl}_{j'l'}(r). \tag{13}$$

To obtain ratios of partial widths using Eq. (13) in our model calculation, we extrapolate the value $R^{jl}_{j'l'}(r)$ at some r to the one at infinity. To see the stability of the value, we plotted the values for all $j \neq j' = \mathrm{D}\bar{\mathrm{D}}$ against the radial distance r for the case of $\lambda = 0.2$ and Y=0.30 as the example in Fig. 1. Because of the oscillation of some ratio as seen in the figure, the channel radii should be set at a farther distance than 200 GeV^{-1} for all ratios to have their asymptotic values. In our following prediction, we take the ratio at $r = 230$ GeV^{-1}. Once the total decay width of a resonant state is obtained as an imaginary part of the complex energy eigenvalue of the complex-scaled coupled channel equation, partial decay widths are obtained from the value of the total width and Eq. (10) for all j and j'.

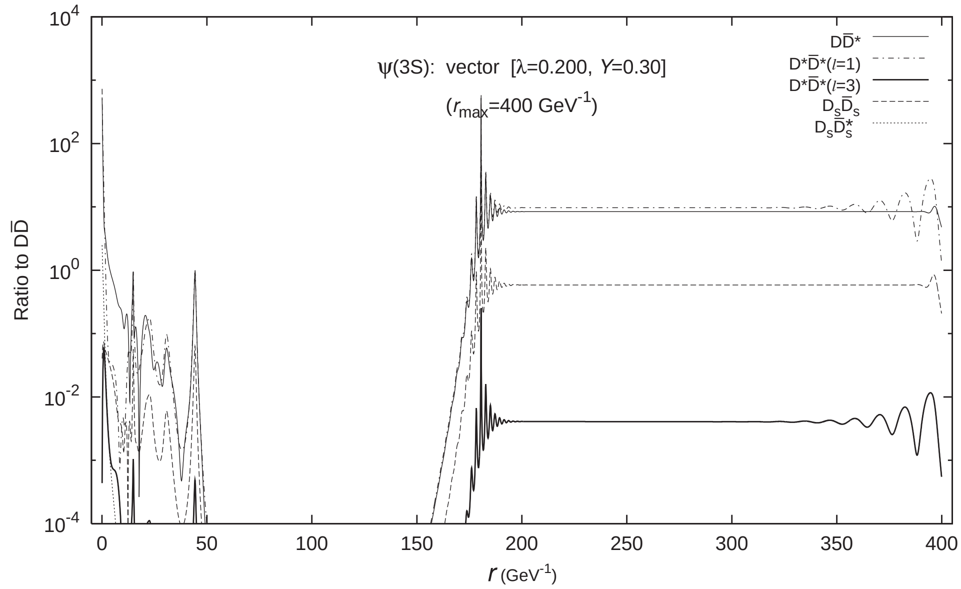

Fig. 1: $R^{jl}_{11}(r)$ in Eq. (13) plotted against the channel radius r in the case of ψ(3S). Here, those for the $D^*_s\bar{D}^*_s$-channel are not shown because of its negligibly small contribution.

Table II: Mass, total width and partial decay widths (Γ_1, Γ_2) of the first pole (with the narrowest width) of the Noro-Taylor model having two open channels. Numerical values are given in atomic unit (a. u.).

	mass	total width	Γ_1	Γ_2
Noro-Taylor[15)]	4.7682	1.420×10^{-3}	5.9×10^{-5}	1.361×10^{-3}
Moiseyev 1[13)]	4.7682	1.44×10^{-3}	5.1×10^{-5}	1.368×10^{-3}
Moiseyev 2[13)]	4.7682	1.44×10^{-3}	5.1×10^{-5}	1.370×10^{-3}
Masui et al.[16)]	4.768197	1.420192×10^{-3}	5.111562×10^{-5}	1.369076×10^{-3}
Our prediction	4.768197	1.420200×10^{-3}	5.111592×10^{-5}	1.369084×10^{-3}

As the method of solving our complex-scaled coupled channel Schrödinger equation numerically, we use the renormalized Numerov method[14)] based on the complex coordinate scale transformation. To see reliability of this numerical method and the expression (13), we solved the Noro-Taylor model of a simple two-channel model potential.[15)] The radial Hamiltonian of this model is given as

$$H^{\text{N-T}} = -\frac{\mathrm{d}^2}{\mathrm{d}\,r^2} + \begin{pmatrix} -1.0 & -7.5 \\ -7.5 & 7.5 \end{pmatrix} r^2 \mathrm{e}^{-r} + \begin{pmatrix} 0 & 0 \\ 0 & 0.1 \end{pmatrix} \tag{14}$$

The model has been well investigated by several other methods[13),15),16)] to demonstrate their usefulness of evaluating partial widths. We have calculated masses, total decay widths, and partial widths (Γ_1 and Γ_2) of 12 lower lying states. Our result shows a very good agreement with previous calculations, especially with the one by the complex scaled Jost function method[16)] for all of the 12 pole-states. As an example, our result for the first resonant pole referred to in Ref. 16) is shown and compared with those obtained by other methods in Table II. Thus our method has turned out to be very encouraging.

3　Numerical results

Parameters λ, m_c and Y are fixed to be $\lambda = 0.20\,\text{GeV}^2$, $m_c = 1.72\,\text{GeV}$, $Y = 0.30$ so as to reproduce overall data of ψ-states, while using $\alpha_{c\bar{c}} = 0.52$, $m_u = m_d = 0.33$ GeV, and $m_s = 0.45\,\text{GeV}$, as was set in our previous analyses.[8)] These are less important parameters since the confining force dominates over the one-gluon-exchange force, and $m_u = m_d$ and m_s enter only in obtaining tran-

Table III: Feature of the traditional ψ-states: mass M, total decay width Γ and main partial-decay width $\tilde{\Gamma}_i$. This quantity $\tilde{\Gamma}_i$ is derived by removing the k^3-phase space factor from the partial decay width Γ_i. An index i distinguishes decaying channels as follows: i=1 for $D\bar{D}$, 2 for $D\bar{D}^*$ and 3 for $D^*\bar{D}^*$. Quantities $\tilde{\Gamma}_1$ and $\tilde{\Gamma}_3$ are given in relative to $\tilde{\Gamma}_2$, while M and Γ are in MeV.

	Experimental data				Model prediction			
	M	Γ	$\tilde{\Gamma}_1/\tilde{\Gamma}_2$	$\tilde{\Gamma}_3/\tilde{\Gamma}_2$	M	Γ	$\tilde{\Gamma}_1/\tilde{\Gamma}_2$	$\tilde{\Gamma}_3/\tilde{\Gamma}_2$
$J/\psi(1S)$	3097	0			3097	0		
$\psi(2S)$	3686	0			3660	0		
$\psi(3770)$	3771	23±2.3			3807	11		
$\psi(4040)$	4039	80±10	0.05±0.03	32.0±12.0	4033	66	0.040	37
$\psi(4160)$	4153	103±8			4214	91	0.052	137

sition potentials through the wave functions of decaying charmed and anti-charmed mesons. Taking the scale angle θ in the complex rotation plane to be 0.65 rad, we have solved our scaled coupled channel equation. The mass, total decay width and partial width prediction for traditional ψ-states are shown in Table III.

The predictions for the traditional ψ-states satisfactorily match the experimental data, considering the fact that our model neglects spin-dependent forces like LS and tensor forces. Above all, ψ(4040)'s feature of mass and partial decay widths, which have been viewed with great attention historically, is reproduced well. Its mass has been hardly reproduced. The single $c\bar{c}$ channel model tends to give a quite larger mass, and by the effect of coupling to open decay channels and the repulsive meson-anti-meson force in 1^- channel, the single channel mass becomes smaller.[8),17)] Prediction of each partial decay width is listed in Table IV. In our coupled channel model, a ψ-state is expressed as a superposition of S, D, $D\bar{D}$, $D\bar{D}^*$, $D^*\bar{D}^*$(l = 1, and l = 3) channels and so on. The probalbility of dominant channels of the traditional ψ-states is listed in Table V. These show that the usual nomination of the traditional ψ-states as being nL(n: principal quantum number, L: orbital angular momentum) of $c\bar{c}$ is appropriate.

The model predicted ψ(3770) is predominantly of D-wave but contains a finite amount of S-wave components. This makes a finite e^+e^- decay width, consistent with the experimental data.[18)] Of 2D, the partial decay width data

Table IV: Model prediction of dominant partial decay widths. Masses and widths are given in MeV.

	M	Γ	$D\bar{D}$	$D\bar{D}^*$	$D^*\bar{D}^*$ (l=1)	$D^*\bar{D}^*$ (l=3)
1D	3807	11	11	0	0	0
3S	4033	66	2	23	39	~0
2D	4214	91	~0	1	6	82

is not known, but our model predicts that it is dominated by the $D^*\bar{D}^*$ decay over both $D\bar{D}$ and $D\bar{D}^*$ as in the 3S case. However, the l-dependence of $D^*\bar{D}^*$ is quite different between 3S and 2D; the l=1 component of the $D^*\bar{D}^*$ decay is dominant for 3S, while the l=3 is dominant for 2D. Our prediction of a small $D\bar{D}$ width of the 2D-state contrasts with results of $\Gamma^{(2D)}_{D\bar{D}}/\Gamma \sim 0.5$ by Alcock et al.[19)] and 0.4-0.5 by Bradley-Robson.[20)] The 2D-state, as shown in Table V, contains an S-wave $c\bar{c}$ component as large as 32%. This is favorable since it has a much larger e^+e^- width than one would expect for a pure D-wave $c\bar{c}$ state.

4 Origin of the ψ(4040) and ψ(4160) states

We have inquired the origin of these coupled channel states. For this purpose, we calculated masses of the $c\bar{c}$ single channel solutions and complex energy eigenvalues of the coupled channel equation in which the strength of the transition potential is gradually and finally decreased to zero. Thus we know the origin of the coupled channel solutions. The 1S, 2S and 1D ψ-states are found to

Table V: Mixing components of the S-/D- wave and those of the meson-antimeson channel in the present ψ-state wave-function (7). Integrated numbers of $\left|b^L(r)\right|^2$ or $\left|u^l_j(r)\right|^2$ over r are shown in percentage(%). Masses and total widths Γ are given in MeV.

Nomination	Mass	Total width	S-wave	D-wave	$D\bar{D}$	$D\bar{D}^*$	$D^*\bar{D}^*$	
nL							(l=1)	(l=3)
1S	3097	0	96	0		1	2	
2S	3660	0	79	6	2	6		
1D	3807	11	21	72				
3S	4033	66	79	6	1	3	8	
2D	4214	91	32	63				3

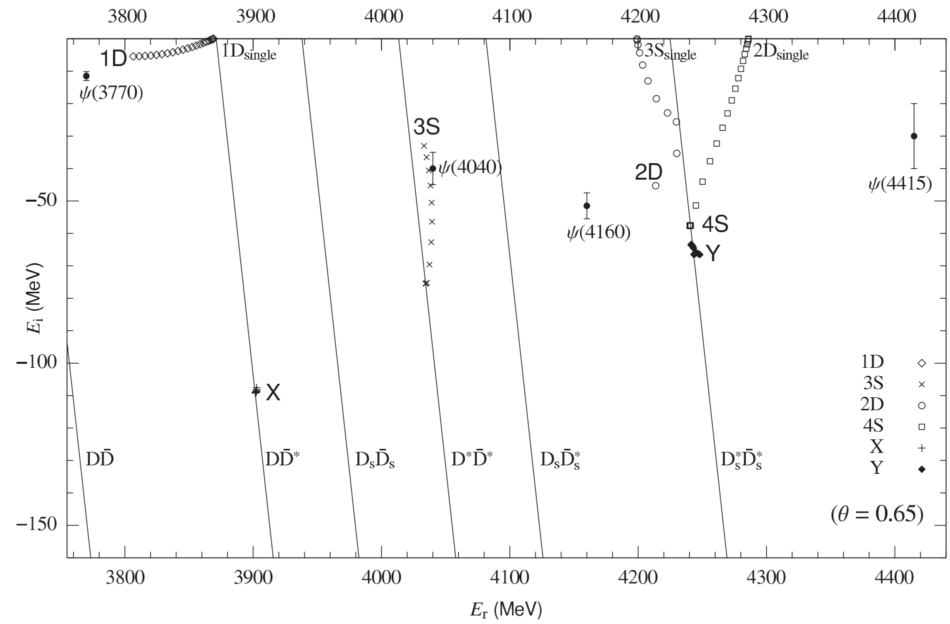

Fig. 2: The complex energy plane shows a dependence of ψ-masses($E_{\rm r}$) and widths($\Gamma = -2E_{\rm i}$) on the strength parameter f of the transition potential in the case of the vector confinement coupling. Here, f is gradually varied through 1.0 to 0.0.

be reduced to their respective $c\bar{c}$ single channel states. The situation for resonant states above the open channel threshold is depicted in Fig. 2.

As seen from Fig. 2, we understand that the controversial state ψ(4040), usually assigned as ψ(3S), may be a remnant of $D^*\bar{D}^*$ state,[21),22)] to our surprise. That is, the seat arises from a $D^*\bar{D}^*$ state, not from a $c\bar{c}$ state. By changing the parameter Y, we have confirmed that this situation is very stable.

The following question arises. What is the state that turns out to be the 3S solution of the single $c\bar{c}$ channel equation when the open channel coupling is switched off? The answer is the 2D-state; it is brought about from $c\bar{c}$ single channel 3S. The 2D is the ruin of the state that was assigned to 3S in the $c\bar{c}$ single channel. The similar situation will appear above the 2D mass region. The relation between the coupled- and the single-channel solutions for the traditional ψ-states are summarized in Table VI.

Our predictions of ratios of partial decay widths for 3S and 2D are listed and compared with those obtained by other previous analyses in Fig. 3. These predictions for the ψ(2D) are very dispersive. As we have no data on the 2D partial decays, experiments on partial decays of the ψ(2D) are highly anticipated.

Table VI: The relation between the coupled- and the single-channel solutions by parameter set of $\lambda = 0.20\,\mathrm{GeV}^2$, $Y = 0.30$, $m_c = 1.72\,\mathrm{GeV}$. M and M_0 denote the masses of the coupled-channel- and the single channel-solutions, respectively. The column [uncoupled] refers to the state of the uncoupled solution. Masses and widths are given in MeV.

Name	nL	Model prediction						Expt. data	
		M	Γ	$c\bar{c}$ probability		M_0	[uncoupled]	M	Γ
$J/\psi(1S)$	$1S$	3097		96%S	0%D	3115	$1S$	3097	0
$\psi(2S)$	$2S$	3666	0	79%S	6%D	3743	$2S$	3686	0
$\psi(3770)$	$1D$	3807	11	21%S	72%D	3869	$1D$	3770	23±3
$\psi(4040)$	$3S$	4033	66	79%S	6%D	4037	$D^*\bar{D}^*$	4040	80±10
$\psi(4160)$	$2D$	4214	91	63%D	32%S	4199	$3S$	4159	103±8

Table VII: Our model predictions of ψ-states other than those in Table VI. Masses and widths are given in MeV.

Name	nL	Model prediction						Expt. data	
		M	Γ	$c\bar{c}$ probability		M_0	[uncoupled]	M	Γ
Y(4260)	$4S$	4248	133	74%S,	17%D	4286	$2D$	4259	88±23±5
$\psi(4415)$	$5S$	4561	30	91%S,	4%D	4587	$4S$	4415	60±20
X(3940)	/	3903	216	56%S,	10%D		$D\bar{D}^*$	3943	<52

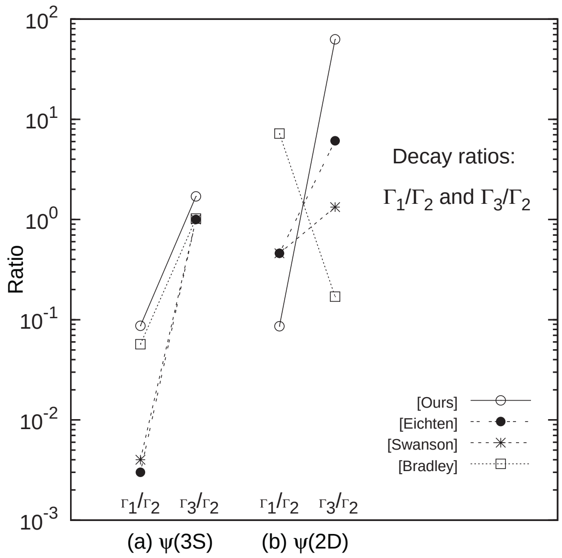

Fig. 3: Ratios of partial widths among decays to $D\bar{D}(\Gamma_1)$, $D\bar{D}^*(\Gamma_2)$ and $D^*\bar{D}^*(\Gamma_3)$ from (a) $3S$ and (b) $2D$. Our prediction is compared with those obtained by Eichten et al.,[7)] Swanson et al.[5)] and Bradrey-Robson.[20)]

5 Discussions

Backed by the success of the present model for the traditional ψ-states, we first discuss some other states obtained by our coupled channel equation. Two 1^{--} solutions appear around $M \sim 4240$–4250 MeV and $\Gamma \sim 120$–130 MeV. One with a smaller mass lies very near the $D_s^*\bar{D}_s^*$ cut and does not show theta independence.[1] The other solution with $M \sim 4250$ MeV and $\Gamma \sim 130$ MeV, being a little apart from the $D_s^*\bar{D}_s^*$ cut is θ-independent. This solution is a candidate of Y(4260)[23)] whose mass and the total decay width is 4259 MeV (88±23±5 MeV). These two solutions may correspond to one physical state. It may be the $\psi(4S)$[24)] noting that the $c\bar{c}$ component is found to be 74% in S-wave and 17% in D-wave, and that the solution with a smaller mass goes to a $c\bar{c}$ state with L=2 with mass about 4286 MeV though the other solution goes to a $D_s^*\bar{D}_s^*$ continuum when the open channel coupling is turned off.

We have another solution at around $M \sim 4560$ MeV and $\Gamma \sim 30$ MeV. This will be a candidate for the experimentally observed $\psi(4415)$. The dominant components are calculated to be 91%S and 4%D. Usually, this state has been assigned as $\psi(4S)$. By the naive potential model, the leptonic width is predicted to be larger by more than factor 2 of the observed value. Hence, $\psi(5S)$ assignment could be a possibility. The mass turns out to be much larger than the data, but we don't consider this a

[1] Due to the nearby $D_s^*\bar{D}_s^*$ continuum, we cannot obtain the θ-independent information and therefore we cannot obtain the right resonance properties. It is considered to be dominant in S-wave.

serious problem since there will be some other open decay channels and we can expect that relativistic effect and spin dependent forces will reduce it.

A solution exists near the mass region of X(3940)[25] as seen in Fig. 2. Although the predicted total decay width is very large compared with the data, we identify this state as X(3940). The model masses of this state and the 1*D*-state is close and they seem to repel to each other. It may be possible that the imaginary part of energy eigenvalue of model X(3940) will be reduced when the spin dependent forces are taken into account and the 1*D*-state mass becomes smaller.

We summarize our model predicted states other than those traditional ψ-states, and their possible assignments in Table VII.

ACKNOWLEDGEMENTS

The authors wish to thank Prof. K. Katō of Hokkaido University for his interest and valuable discussions regarding this work.

REFERENCES

1) A. Le Yaouanc, L. Oliver, O. Pène and J. -C. Raynal, Phys. Lett. B **71** (1977), 397.

2) A. Le Yaouanc, L. Oliver, O. Pène and J. -C. Raynal, Phys. Lett. B **72** (1977), 57.

3) For the recent review of the OZI decay analyses of charmonium states, see E. S. Swanson, Phys. Rep. **429** (2006), 243.

4) S. Okubo, Phys. Lett. **5** (1963), 165.
G. Zweig, CERN Report No. 8419/Th (1964), 412(unpublished).
I. Iizuka, K. Okada and O. Shito, Prog. Theor. Phys. **35** (1966), 1061.

5) For the recent analysis by the refined $^3P_0$ model, see T. Barnes, S. Godfrey and E. S. Swanson, Phys. Rev. D **72** (2005), 054026.

6) E. Eichten, K. Gottfried, T. Kinoshita, K. D. Lane and T. M. Yan, Phys. Rev. Lett. **36** (1976), 500; Phys. Rev. D **17** (1978), 3090; **21** (1980), 203.

7) E. Eichten, K. Lane and C. Quigg, Phys. Rev. D **73** (2006), 014014.

8) N. Yabusaki, K. Katō, M. Hirano, M. Sakai and Y. Matsuda, Few-Body Systems **28** (2000), 1.

9) J. Aguilar and J. M. Combes, Commun. Math. Phys. **22** (1971), 269.
E. Balslev and J. M. Combes, Commun. Math. Phys. **22** (1972), 280.
B. Simon, Commun. Math. Phys. **27** (1972), 1.
For review of the complex scaling method, see Y. K. Ho, Phys. Rep. **99** (1983), 1.

10) N. Yabusaki, M. Hirano, K. Katō, M. Sakai and Y. Matsuda, Prog. Theor. Phys. **106** (2001), 389.

11) Pedro J. de A. Bicudo and Jose E. F. Ribiero, Phys. Rev. D **42** (1990), 1611.

12) A. Amer, A. Le Yaouanc, L. Oliver, O. Pène and J. -C. Raynal, Phys. Rev. Lett. **50** (1983), 87.
A. Le Yaouanc, S. Ono, L. Oliver, O. Pène and J. -C. Raynal, Phys. Rev. D **29** (1984), 1233.
A. Le Yaouanc, L. Oliver, O. Pène and J. -C. Raynal, Phys. Rev. D **31** (1985), 137.

13) N. Moiseyev and U. Peskin, Phys. Rev. A **42** (1990), 255.

14) B. R. Johnson, J. Chem. Phys. **67** (1977), 4086; **69** (1978), 4678.

15) T. Noro and H. S. Taylor, J. of Phys. **B13** (1980), L377.

16) H. Masui, S. Aoyama, T. Myo and K. Katō, Prog. Theor. Phys. **102** (1999), 1119.

17) M. Hirano, T. Honda, K. Katō, Y. Matsuda and M. Sakai, Phys. Rev. D **51** (1995), 2353.

18) Particle Data Group, J. of Phys. **G33** (2006), 765.

19) J. W. Alcock, M. J. Burfitt and W. N. Cottingham, Z. Phys. **C25** (1984), 161.

20) A. Bradley and D. Robson, Phys. Lett. B **39** (1980), 69.

21) M. B. Voloshin and L. B. Okun, JETP Lett. **23** (1976), 333.

22) A. De Rújula, H. Georgi and S. L. Glashow, Phys. Rev. Lett. **37** (1976), 398; **38** (1977), 317.

23) B. Aubert et al., (BABAR Collaboration), Phys. Rev. Lett. **95** (2005), 142001.
T. E. Coan et al., (CLEO Collaboration), Phys. Rev. Lett. **96** (2006), 162003.
K. Abe et al., (Belle Collaboration), BELLE-CONF-0610, hep-ex/0612006(2006).

24) E. J. Llanes-Estrada, Phys. Rev. D **72** (2005), 031503 (R).

25) K.Abe et al., (Belle Collaboration), Phys. Rev. Lett. **98** (2007), 082001[arXiv: hep-ex/0507019].

（平野 雅宣　札幌校教授）
（松田 康夫　酪農学園大学非常勤講師）
（酒井 源樹　旭川校教授）